ELSEVIER

Ceramics International 32 (2006) 713–718

CERAMICS INTERNATIONAL

www.elsevier.com/locate/ceramint

WO_3 and ZnO-doped SnO_2 ceramics as insulating material

M.A.L. Margionte, A.Z. Simões *, C.S. Riccardi, F.M. Filho, A. Ries, L. Perazolli, J.A. Varela

Chemistry Institute, Universidade Estadual Paulista, UNESP, Rua Prof. Francisco Degni s/n, 14801-970 Araraquara, SP, Brazil

Received 3 January 2005; received in revised form 15 April 2005; accepted 25 May 2005
Available online 26 July 2005

Abstract

SnO_2 ceramics doped with ZnO and WO_3 were prepared by mixed oxide method. The effect of ZnO and WO_3 additives could be explained by the substitution of Sn^{4+} by Zn^{2+} and W^{6+}. The addition of WO_3 inhibits the grain growth due to the segregation of $SnZnWO_8$ and $ZnWO_6$ at the grain boundaries without strong influence on the densification process. The electrical characterization ($\log E \times \log J$) shows that the ternary system SnO_2–ZnO–WO_3 exhibits a very high resistivity of around 10^{14} Ω m. Independently of the WO_3 concentration, the electrical conductivity of the SnO_2–ZnO–WO_3 system is always lower than that of the undoped tin dioxide.

Keywords: A. Sintering; E. Insulators; Tin dioxide

1. Introduction

Tin dioxide (SnO_2) is an n-type semiconductor with rutile type crystal structure [1]. When sintering SnO_2 powder, the final bodies normally have low densities. A high oxygen diffusion coefficient, present even at low temperatures, and the stability of the Sn(II) oxidation state promote oxygen losses according to Eq. (1) [2]. Dense SnO_2-based ceramics can be achieved by introducing dopants or by hot isostatic pressure processing [3–6]. The function of the ZnO dopant is the creation of oxygen vacancies and Zn''_{Sn} defects according to Eq. (2). The latter contribute to the Schottky barrier formation and lead to a highly dense material [7]. The addition of WO_3 decreases the conductivity of the varistors when the solid solution is obtained, due to the resulting tin vacancies (Eq. (3)), that act as acceptor levels compensating the intrinsic n-conductivity of SnO_2, through decreasing the electron density in the conduction band.

When SnO_2 is appropriately doped, both, dopants and defects may accumulate at the grain boundaries, thus creating a potential barrier. Such ceramics exhibit then varistor behavior, i.e. a nonlinear current–voltage characteristic as previously presented [8–10]. In the present article we consider the possibility, that tungsten is precipitated at the grain boundaries and promotes the formation of potential barrier according to the Eq. (3):

$$SnO_{2(s)} \overset{1200^{\circ}C}{\longleftrightarrow} SnO_{(g)} + \tfrac{1}{2}O_{2(g)} \quad (1)$$

$$ZnO \overset{SnO_2}{\longrightarrow} Zn''_{Sn} + V_0^{\bullet\bullet} + O_0^x \quad (2)$$

$$2WO_3 \overset{SnO_2}{\longrightarrow} 2W''_{Sn} + V_{Sn}^{\bullet\bullet\bullet\bullet} + 6O^x \quad (3)$$

Finally, we report the effect of ZnO and WO_3 additives on the morphological and electrical properties of SnO_2 ceramics. The results demonstrate that such ceramics may find future applications as high resistance materials.

2. Experimental

The powder was prepared using the mixed oxide method in alcoholic medium. All the used oxides were analytical grade: SnO_2 (Cesbra/Br), ZnO (Auricchio/Br), WO_3 (Alfa Aesar). The molar composition of the investigated system was SnO_2 doped with ZnO with concentrations of 1.0 and 2.0 mol% and WO_3 from 0.005 to 0.01 mol%.

* Corresponding author. Tel.: +55 16 201 6707; fax: +55 16 222 7932.
E-mail address: alezipo@yahoo.com (A.Z. Simões).

0272-8842/$30.00
doi:10.1016/j.ceramint.2005.05.008

Table 1
Influence of ZnO and WO_3 additives on the initial sintering temperature (T_{is}), maximum sintering temperature (T_{max}), relative densities (ρ) and average grain size (G)

System	T_{is} (°C)	T_{max} (°C)	ρ (%)	G (μm)
SnO_2 + 1.0% ZnO	876	1174	98.0	10.2
SnO_2 + 1.0% ZnO + 0.005% WO_3	876	1194	96.6	5.9
SnO_2 + 1.0% ZnO + 0.01% WO_3	865	1221	95.3	5.7
SnO_2 + 1.0% ZnO + 0.1% WO_3	906	1152	95.5	6.3
SnO_2 + 2.0% ZnO	859	1236	97.1	6.2
SnO_2 + 2.0% ZnO + 0.005% WO_3	861	1233	96.2	5.6
SnO_2 + 2.0% ZnO + 0.05% WO_3	864	1220	94.2	5.4
SnO_2 + 2.0% ZnO + 0.01% WO_3	856	1236	95.6	5.2
SnO_2 + 2% ZnO + 0.1% WO_3	876	1250	95.8	5.7

Appropriate stoichiometric quantities of the starting materials where thoroughly mixed in ethanol medium by ball milling. Next, the dried powder mixture was pressed into pellets by uniaxial pressing followed by isostatic pressing at 210 MPa. No calcination was performed prior to the pellet preparation. These pellets were then sintered for 4 h in dynamic oxygen atmosphere (flux 3 cm^3/min, oxygen purity 95%) at optimized maximum sintering temperatures, which were obtained from dilatometry of the different compositions and are given in Table 1. All heating rates were 5 °C/min, the samples were slowly cooled to room temperature (cooling rate 5 °C/min).

The dilatometric analyses were performed with a Netzsch 402E unit, up to 1500 °C, at a heating rate of 10 °C/min in oxygen atmosphere. The linear retraction and linear retraction rates were collected every 0.5 °C. To obtain the SEM micrographies, the sintered samples were fractured and manual polished using 400, 600 and 1000 SiC papers. After this procedure, they were automatically polished for 4 h using alumina with 0.05 μm particle diameter followed by thermal etching at 1300 °C for 30 min.

To perform TEM/EDS analysis the samples were cutted in 0.3 mm thick disks with a Low Speed Diamond Wheel Saw (Model 650-SBT) and polished until 30 μm thickness.

After this procedure the samples were placed on the sample holder and observed by electron transmission microscopy (Digital Spectrometer-Pinceton Gamma Tech). EDS (energy dispersive spectrometry) analyses were performed in grains, at grain boundaries, triple points and precipitates.

To perform the electrical measurements, silver contacts were deposited on the samples surfaces (silver paint). Current–tension (I–V) measurements were taken using a high voltage measure unit (KEITHLEY Model 237) connected to a computer.

3. Results and dscussion

The influence of ZnO and WO_3 dopants on the sintering process of the SnO-based varistor was investigated by dilatometric analyses. It was observed that the WO_3 addition affects the grain size and the final density of the sintered samples (Table 1). The linear shrinkage rate ($d(\Delta l/l_0)/dT$) and linear shrinkage $\Delta l/l_0$ as a function of temperature for different ZnO and WO_3 concentrations are presented in Fig. 1a and b. It was noted that the densification temperature decreases with an increasing WO_3 concentration due to a higher amount of Sn vacancies according to Eq. (3). These vacancies facilitate material diffusion during sintering. Fig. 1b illustrates the linear shrinkage rate for different ZnO and WO_3 concentrations. From these results it can be verified that the limit to form a ZnO solid solution in the SnO_2 matrix is 1.0 mol%. Here, the maximum shrinkage rate occurred around 1200 °C. The presence of peaks close to 1080 °C for the highly ZnO-doped samples (e.g. 2.0 mol% ZnO as shown in Fig. 1b) indicates the agglomeration during the sintering process (intra and interagglomerates) from particles with different sizes, i.e., SnO_2 (0.09 μm) and ZnO (0.26 μm). These values were determinated before sintering. Another peak close to 1380 °C could arise from defects located at the grain boundaries or from a possible partial evaporation of oxygen in the SnO_2 phase. The initial sintering temperature (T_{is}) and the maxium sintering temperature (T_{max}) are given in Table 1. The increase in

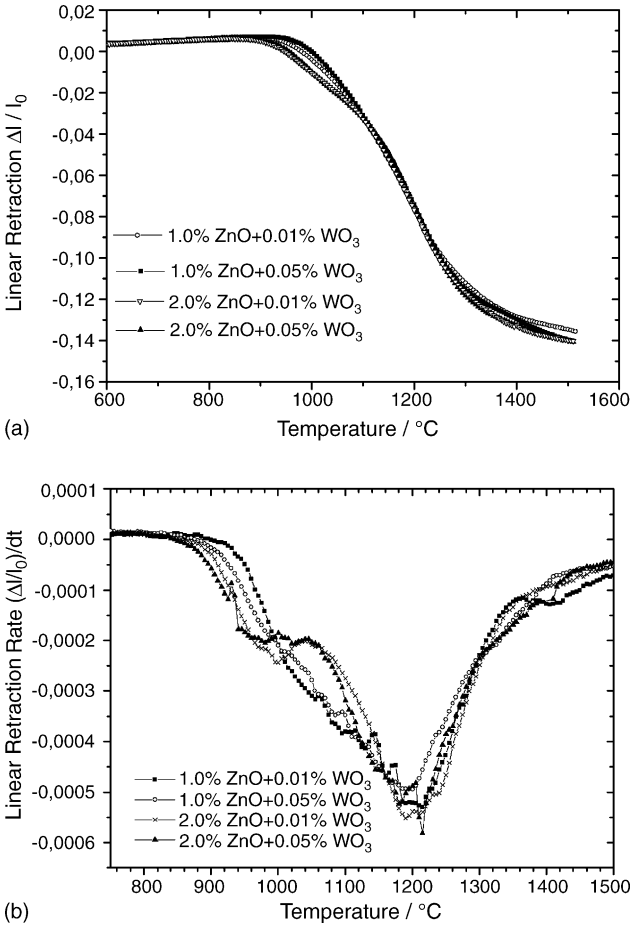

Fig. 1. (a) Linear retraction and (b) linear retraction rate for different dopant concentrations as a function of temperature.

tungsten concentration has strong influence on the sintering process of the system. For the highly doped samples, there is a segregation at the grain boundaries, which leads to a decrease in the grain size. This effect is mainly due to the precipitation of a new W enriched ceramic phase, as discussed in the subsequent sections.

The densities of the samples determined by Archimedes method were evaluated as a function of WO_3 content and are related to the theoretical density of SnO_2 ($\rho_{theoretical}$ = 6.95 g/cm^3; Table 1). The highest values were obtained for the compositions SnO_2 + 1.0 mol% ZnO + 0.1 mol% WO_3 ($\rho > 97\%$) and SnO_2 + 2.0 mol% ZnO + 0.1 mol% WO_3 ($\rho > 95\%$). The final densities after sintering are close to 95%, as shown in Table 1. They were only slightly affected by variations of the WO_3 content, although the average grain size decreased significantly with the addition of WO_3. A dramatic decrease in grain size was also noted for the heavily (2%) ZnO-doped samples even in the absence of tungsten. This indicates that Zn in higher concentrations not only provides oxygen vacancies to facilitate the densification, but also acts as a grain growth inhibitor. This could result in a $SnZnO_3$ phase at the grain boundaries.

Fig. 2 shows SEM images of some tin dioxide ceramics considered in this study. The mean grain size was obtained by the intercept method. The samples doped with 2.0 mol% ZnO present a larger number of pores (intergranulars) compared with the samples doped with 1 mol% ZnO (intergranulars and intragranulars). There are significant differences in the average grain size with the addition of WO_3 probably due to the segregation of $SnZnWO_8$ and $ZnWO_6$ phases at the grain boundaries, which might decrease the grain boundary mobility leading to a decrease in the grain size. These results are consistent with the dilatometer and TEM/EDS analyses. The grains are regularly distributed with an average grain size ranging from 5.2 to 10.2 μm (Table 1).

The mechanism that inhibits densification when WO_3 is added to the system can probably be associated to the reduced amount of oxygen vacancies at grain boundaries according to Eq. (3).

Fig. 3 illustrates the TEM micrographies for the system SnO_2 + 2.0% ZnO + 0.05% WO_3 in different regions of a sample. The points A–C indicate the position where EDS analyses were performed. Fig. 3a shows the formation of two precipitates D_1 and D_2, Fig. 3b the formation of a precipitate D_3. In Fig. 3c a triple point is observed.

Fig. 4 shows the EDS analyses for the composition SnO_2 + 2.0% ZnO + 0.5% WO_3 in different samples region: grain (A), grain boundary (B), triple point (C) and precipitate (D_1, D_2 and D_3). It can be observed that grains and simple grain boundaries mainly consist of SnO_2 while the grain boundaries at the triple point are Zn and W

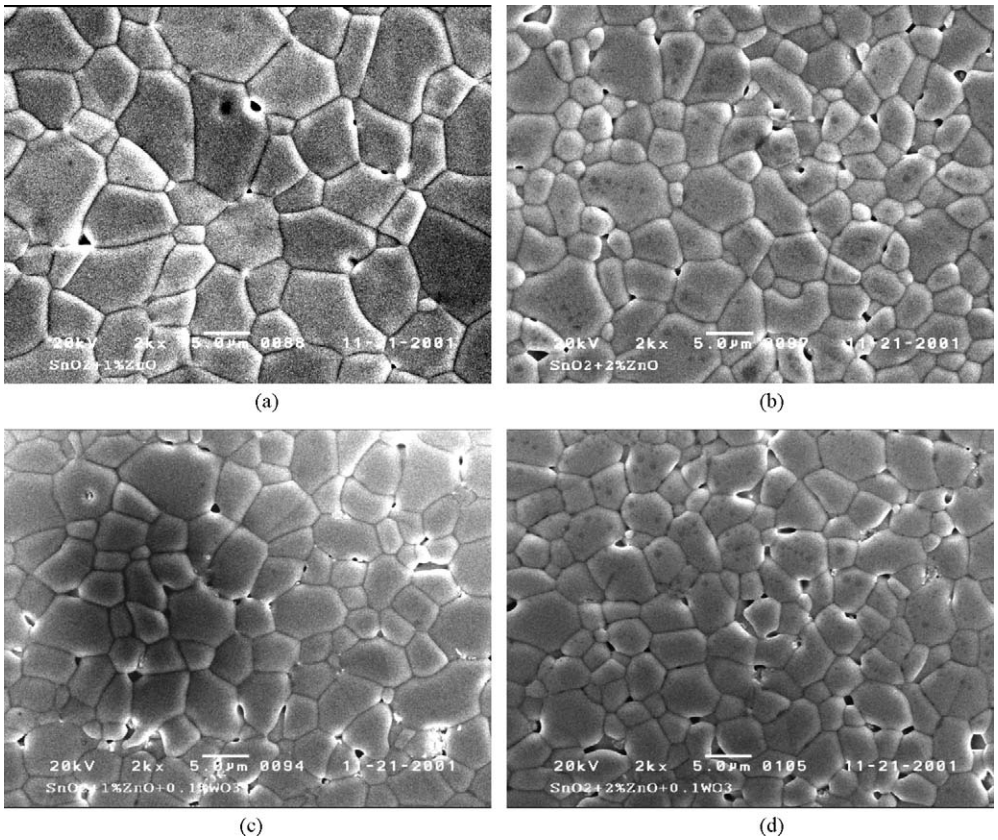

Fig. 2. SEM micrographies for the samples: (a) SnO_2 + 1.0% ZnO; (b) SnO_2 + 2.0% ZnO; (c) SnO_2 + 1.0% ZnO + 0.1% WO_3; and (d) SnO_2 + 2.0% ZnO + 0.1% WO_3.

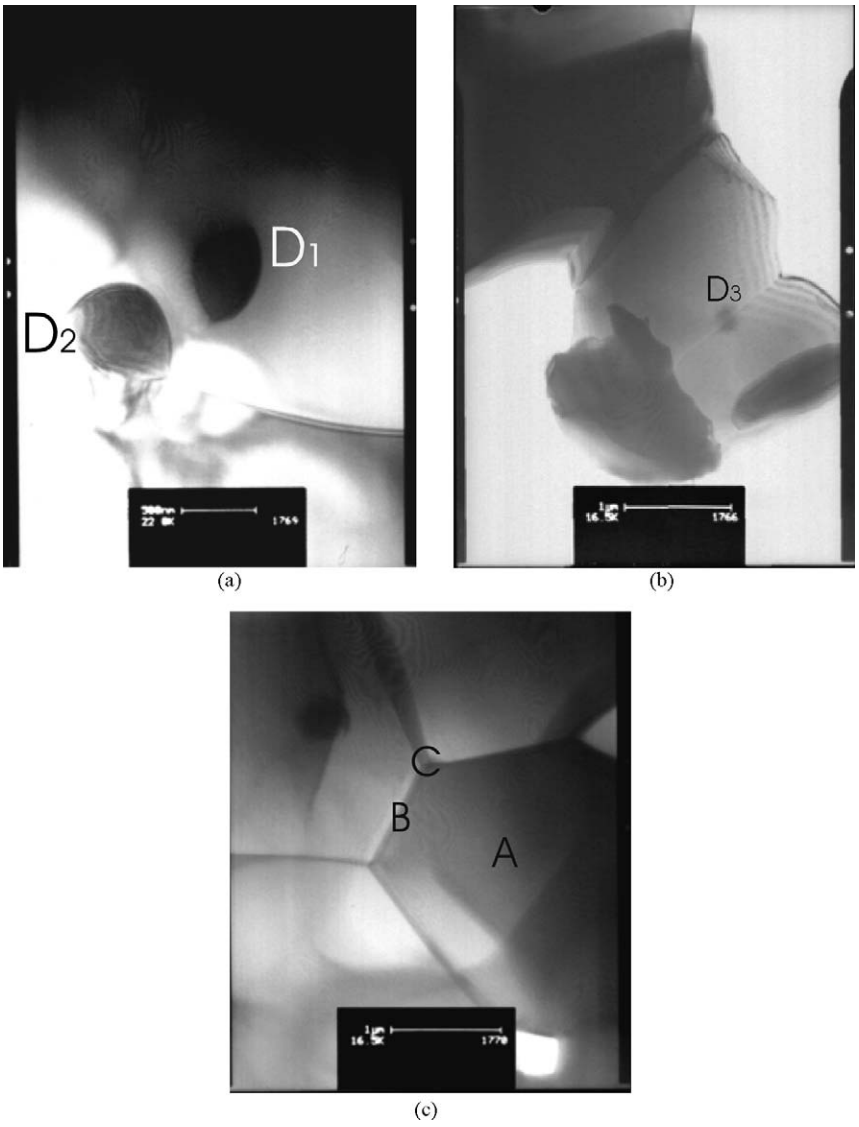

Fig. 3. TEM analyses for the sample SnO_2 + 2.0% ZnO + 0.05% WO_3: (a) precipitates; (b) grain boundary; and (c) triple point.

enriched. It was also found that the precipitates contain a high concentration of dopants. From these results we can confirm that Zn and W segregate at the grain boundaries. It is suggested that the addition of 2.0 mol% ZnO causes a $SnZnO_3$ phase segregation at the grain boundaries due to the substitution of Zn by Sn. This $SnZnO_3$ phase is W enriched, as can be seen from Fig. 4c and d.

Current–voltage measurements as function of WO_3 content and sintering time are presented in Fig. 5a and b, respectively. When fitting the equation $I = KV^{\alpha}$, which describes the current–voltage characteristics for varistors, in the experimental data, all samples have a nonlinear coefficient (α) between 1 and 3 and resistance of above 1 MΩ. Due to this high resistance, the samples cannot be called varistors, although some potential barrier at grain boundaries cannot be neglegted. Above an electric field strength of 10 kV/cm, the electric characterization shows linear, ohmic behavior, indicating a low conductivity of SnO_2 grains.

The addition of WO_3 increases the room temperature resistivity from 3.44×10^7 Ω cm (system SnO_2 + 1% ZnO) to 3.66×10^{12} Ω cm (system SnO_2 + 1% ZnO + 0.1% WO_3). It was confirmed, that the sintering time also influences the resistivity, for 2 h sintering time, the highest value was obtained (Fig. 5b). In order to optimize these ceramics for technical applications, attention should be paid to this fact. The previously discussed segregation of WO_3 and ZnO at the grain boundaries is responsible for the increase in the electric resistivity of the SnO_2·ZnO·WO_3 system, which is close to diamond resistivity, which was not expected at the beginning of this study.

4. Conclusions

The addition of WO_3 inhibits the grain growth of the SnO_2·ZnO ceramic and has moderate detrimental influence

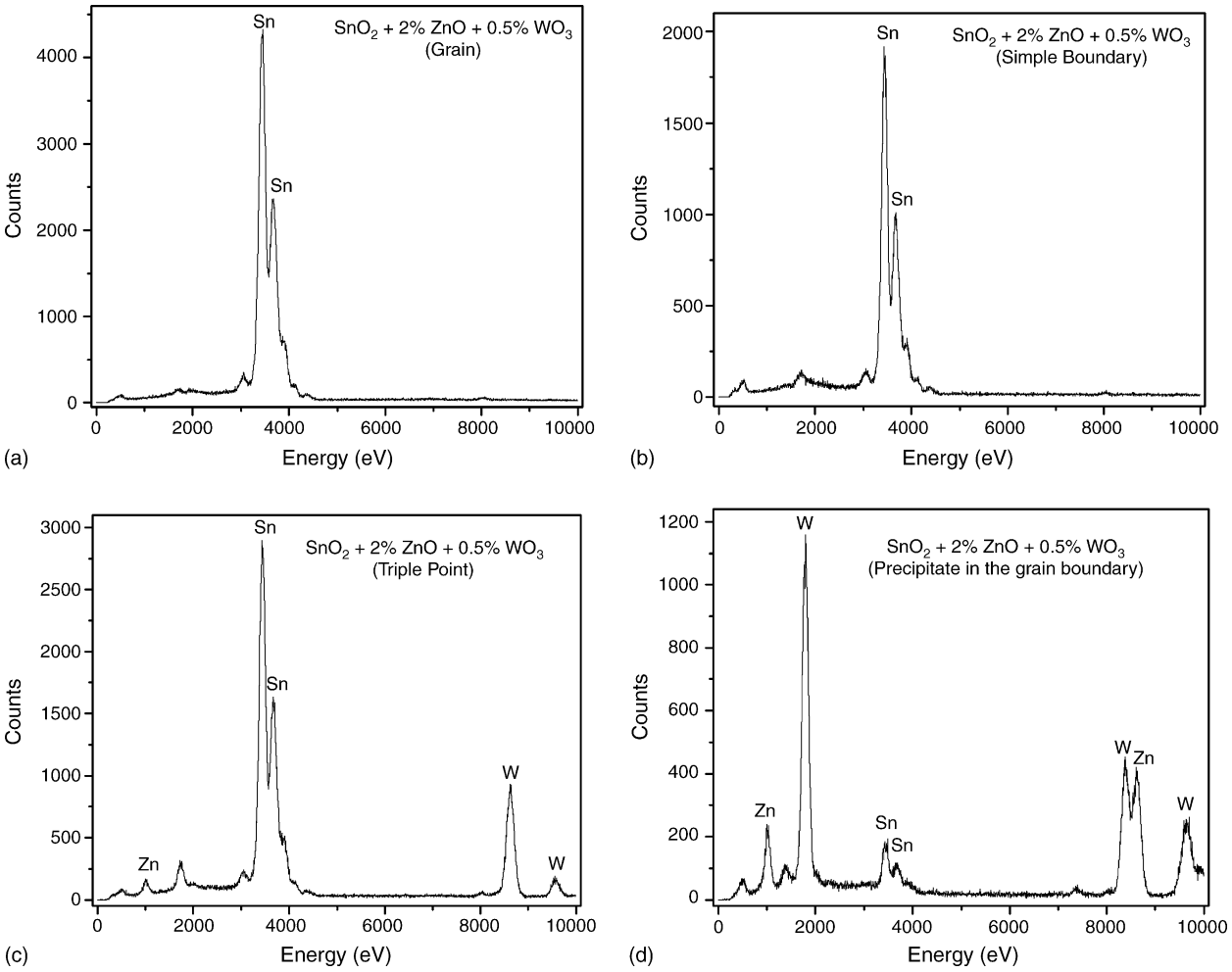

Fig. 4. EDS analyses for the sample SnO_2 + 2.0% ZnO + 0.5% WO_3: (a) grain; (b) grain boundary (c) triple point; and (d) precipitate.

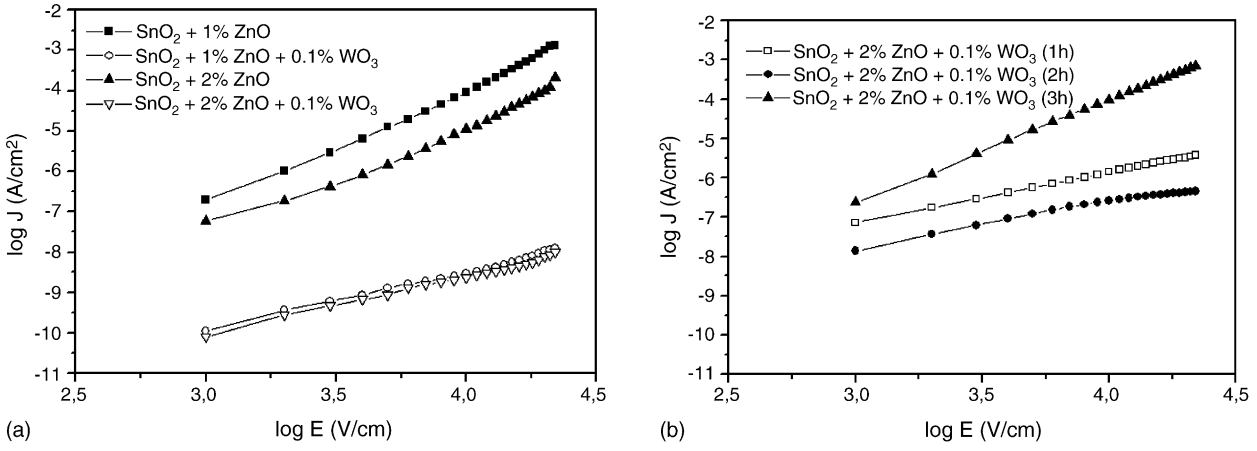

Fig. 5. Applied electric field as a function of current density for different ZnO and WO_3 concentrations (a) and sintering times (b).

on the densification of the system. The segregation of WO_3 is probably responsible for the increase in the electrical resitivity of the SnO_2–ZnO–WO_3 system. These systems have mainly ohmic characteristics and could be used as highly insulating materials.

Acknowledgement

The authors thank to FAPESP, CNPq, CAPES, FINEP and DAAD for the financial support, and to CESBRA for the supply of high purity SnO_2.

References

[1] J.G. Fagan, V.R.W. Amarakoon, Reliability and reproducibility of ceramic sensors: Part III. Humidity sensors, Am. Ceram. Soc. Bull. 72 (1993) 119–130.
[2] S.J. Park, K. Hirota, H. Yamamura, Enhanced sintering of tin dioxide with additives under isothermal condition, Ceram. Int. 10 (1984) 115–116.
[3] J.A. Varela, O.J. Whittemore, E. Longo, Pore-size evolution during sintering of ceramic oxides, Ceram. Int. 16 (1990) 177–189.
[4] T. Kimura, S. Inada, T. Yamaguchi, Microstructure development in SnO_2 with and without additives, J. Mater. Sci. 24 (1989) 220–226.
[5] S.A. Pianaro, P.R. Bueno, E. Longo, J.A. Varela, A new SnO_2 based varistor system, J. Mater. Sci. Lett. 14 (1995) 692–694.
[6] P.R. Bueno, S.A. Pianaro, E.C. Pereira, L.O.S. Bulhoes, E. Longo, J.A. Varela, Investigation of the electrical properties of SnO_2 varistor system using impedance spectroscopy, J. Appl. Phys. 84 (1998) 3700–3705.
[7] D.R. Clarke, Varistor ceramics, J. Am. Ceram. Soc. 82 (1999) 485–502.
[8] L.N. Levinson, H.R. Philipp, Zinc oxide varistor—a review, Ceram. Bull. 65 (1986) 639–646.
[9] T. Masuyama, Effect of cobalt(II) oxide and manganese(IV)oxide on sintering of tin (IV) oxide, Jpn. J. Appl. Phys. 7 (1968) 1294–1298.
[10] M. Matsuoka, Nonohmic properties of zinc oxide ceramics, Jpn. J. Appl. Phys. 10 (1971) 736–745.